Lower-Hybrid Beam-Plasma Instability

R. P. H. Chang
Bell Laboratories, Murray Hill, New Jersey 07974
(Received 19 May 1975)

Experimental and theoretical studies of the nonresonant lower-hybrid beam-plasma instability have been carried out. The instability has a maximum growth rate when the phase velocity of the wave along the magnetic field lines is comparable to the electron thermal velocity. Electron heating associated with this instability has also been observed.

The injection of high-energy neutral beams into tokamaks and mirror machines is of considerable interest for the purpose of auxiliary heating.[1] Theories on possible microinstabilities associated with these systems have also been reported recently.[2] In this Letter I wish to report experimental observations and theoretical analysis of the nonresonant lower-hybrid beam-plasma instability. The experimentally measured properties of the instability are in good agreement with the theory. As the instability developed into saturation electron heating was observed, indicating loss of energy from the ion beam.

I shall first describe the properties of the lower-hybrid beam-plasma instability when an ion beam [with velocity U ($v_i<U<v_e$) which is greater than the ion thermal velocity $v_i=(T_i/M)^{1/2}$ but less than the electron thermal velocity $v_e=(T_e/m)^{1/2}$] traverses a homogeneous plasma at right angles to the confining magnetic field. The main features of the instability are as follows: (1) The characteristic frequency and growth rate are comparable to the lower-hybrid frequency. [Here the parameters are such that the ions are effectively unmagnetized, and so the lower-hybrid frequency is $\omega_{\rm LH}=\omega_{pi}(1+\omega_{pe}^2/\Omega_e^2)^{-1/2}$, where ω_{pi}, ω_{pe}, and Ω_e are the ion plasma frequency, electron plasma frequency, and the electron cyclotron frequency, respectively.] (2) The instability has a maximum growth rate when the phase velocity, $\omega/k_\parallel$, along the magnetic field lines is comparable to the electron thermal velocity. (3) The instability spectral volume (in ω-$\vec{k}$ space) decreases with increasing ion-beam temperature. (4) This instability is insensitive to the change of the electron-ion temperature ratio, T_e/T_i. (5) As the instability develops, plasma heating may take place.[3]

The linear, electrostatic dispersion relation for a homogeneous plasma with an isotropic Maxwellian distribution and an ion beam (also with a Maxwellian distribution) traversing at right angles to the confining field lines is[4]

$$1-(T_e/T_i)(2\bar{k}^2)^{-1}Z'\big((T_e/T_i)^{1/2}(\bar{\omega}/\sqrt{2})\bar{k}^{-1}\big)(1-\eta) - \eta(T_e/T_b)(2\bar{k}^2)^{-1}Z'\big((T_e/T_b)^{1/2}(\bar{\omega}/\sqrt{2})\bar{k}^{-1}-U/\sqrt{2}v_b\big)-(2\bar{k}^2)^{-1}Z'\big((\bar{\omega}/\sqrt{2})\bar{k}^{-1}\bar{\theta}^{-1}\big)=0,$$

where $\bar{\omega}=\omega/\omega_{\rm LH}$, $\bar{k}=\tilde{k}(\Omega_e/\omega_{pe})(1+\omega_{pe}^2/\Omega_e^2)^{1/2}$, $\tilde{k}=k_\perp\rho_e$, T_b is the ion-beam temperature, $\eta=N_b/N_0$ is the beam-to-plasma density ratio, $\bar{\theta}=(k_\parallel/k)\times(M/m)^{1/2}$, v_b is the beam thermal velocity, U is the beam velocity, and Z' is the derivative of the plasma dispersion function. In arriving at this dispersion relation I have assumed the following: (1) $\Omega_i\ll|\omega|\ll\Omega_e$; (2) $k_\perp\rho_i\gg1$, where ρ_i is the ion gyroradius; (3) $k_\parallel\rho_e\ll1$ and $k_\perp\rho_e\ll1$, where ρ_e is the electron gyroradius. This dispersion relation has been numerically analyzed on the computer for various parameters of interest to the present experiments. McBride *et al.*[3] have recently made a detailed theoretical study of a similar dispersion relation for the case of relative streaming of electrons and ions across a magnetic field but without a beam. Figure 1(a) shows a typical plot of the maximum growth rate (maximized over $\bar{k},\bar{\omega}$) $\gamma^*/\omega_{\rm LH}$ versus $\bar{\theta}$ for different values of beam velocities. From these plots we find that the maximum growth rate occurs when $\omega/k_\parallel$ is comparable to the electron thermal velocity, in agreement with previous investigations.[3] We also note that the spectrum of instability is generally quite broad, extending from the region of resonant lower-hybrid waves ($\bar{\theta}\lesssim0.2$) to nonresonant lower-hybrid waves ($\bar{\theta}\lesssim3$), and finally damps out after passing through the region of ion acoustic waves ($\bar{\theta}>3$). However, as the spread of the

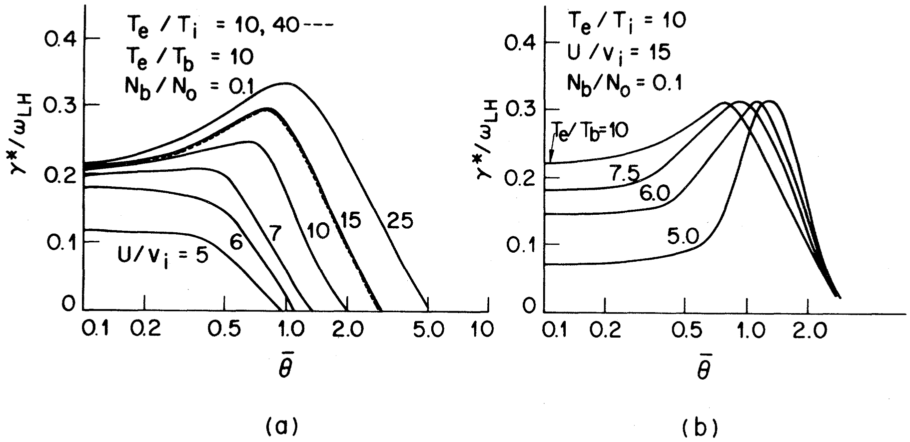

FIG. 1. Plots of the maximum growth rate versus $\bar{\theta}$ (a) for different values of U/v_i and (b) for different values of T_e/T_b.

beam width is increased (i.e., its temperature) we see in Fig. 1(b) that the instability region decreases. For waves with small $\bar{\theta}$ the growth rate is more sensitive to the change of the slope of the beam distribution and thus decreasing the slope (i.e., increasing the beam temperature) decreases the growth rate. However, we notice in Fig. 1(a) that the instability is not sensitive to changes in the electron-ion temperature ratio.

Physically, we can view the instability evolving in the following way. The slow space-charge wave on the ion beam is a wave which carries negative energy; i.e., when the beam passes through a lossy medium (in the present case electron Landau damping along the magnetic field lines), energy is extracted from this wave causing it to grow in amplitude. Since the growth rate of the instability is maximum when the parallel-wave phase velocity of the nonresonant mode is of the order of the electron thermal velocity, we expect efficient energy transport from the beam to the bulk of the electrons via Landau damping.

The experiments were performed with the Bell Telephone Laboratories linear plasma device; its properties and plasma parameters have been described previously.[5] In the present experiment the following plasma parameters were used: density, $N_0=(5-50)\times 10^9$ cm^{-3}; magnetic field, $B_0 \leq 500$ G; temperatures, $T_e=3-7$ eV, $T_i \leq 0.2$ eV for helium, neon, and argon gases. The plasma was collisionless for the waves studied. A sketch of the experimental setup is shown in Fig. 2(a). The main plasma column was 200 cm long and approximately 14 cm in diameter. A separate plasma was produced adjacent to the main plasma column for the purpose of ion-beam extraction. The two plasmas, which could be held at independent plasma potentials, were separated by a fine, negatively biased grid of 5 cm in width and an adjustable length, $L \leq 100$ cm. An array of n beams (in the sketch, $n=4$) was also made such that each beam had a length $l=L/n$. This was done to impose a fixed value of $k_\parallel$ in the experiment. The beam voltage could be varied up to 100 V, while the operating beam density was $N_b/N_0 \leq 0.1$. From electrostatic-energy-analyzer measurements, it was found that the ion beam

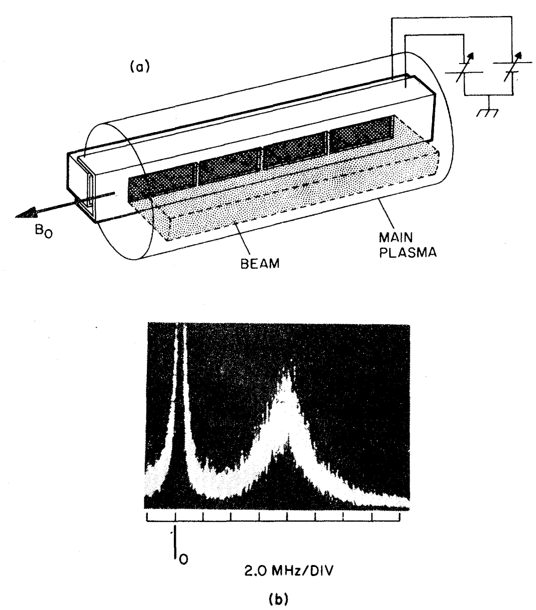

FIG. 2. (a) Simplified schematic of the experimental setup. (b) Instability spectrum for argon plasma.

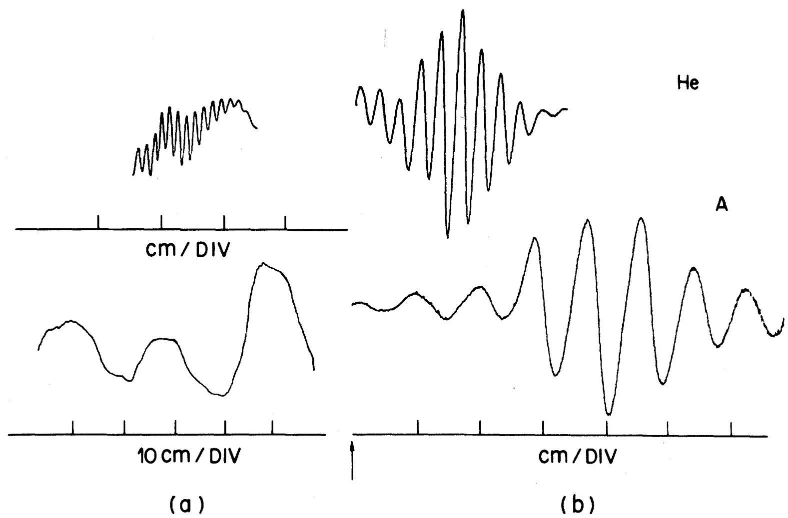

FIG. 3. (a) Interferometer trace for $\lambda_\perp$ (top) and $\lambda_\parallel$ (bottom) of the unstable mode corresponding to Fig. 2. (b) Interferometer traces of $\lambda_\perp$ for He (top) and Ar (bottom); the arrow indicates the location of the ion-beam source.

had an energy spread of $\Delta V_0/V_0 \simeq 0.04$. Figure 2(b) shows a typical spectrum for the case of argon gas when the plasma parameters ($\omega_{pe}/\omega_{ce} \simeq 1$, $U/v_i \simeq 15$, $T_e/T_i \simeq 40$, $T_e/T_b \simeq 5$, and $N_b/N_0 \simeq 0.05$) were adjusted for maximum instability growth rate. Similar spectra were also observed for helium and neon gases. Interferometer traces of the most unstable mode corresponding to that of Fig. 2(b) are shown in Fig. 3(a). The perpendicular wavelength is given by the top trace, while the wavelength (here l was adjusted to be 20 cm, and there was an array of three beams) along the field lines is given by the bottom trace. From these measurements and the plasma parameters, we find $(k_\parallel/k)(M/m)^{1/2} \simeq 1.5$, $\omega/k_\parallel \simeq v_e \simeq 10^8$, and $\omega/\omega_{\rm LH} \cong 1.5$, in good agreement with the predictions of the linear theory for maximum growth rate. As the beam penetrates into the plasma we expect the unstable mode to grow in space for a distance comparable to the ion-beam gyroradius, beyond which it starts to damp. This behavior was observed by measuring the unstable wave amplitude with a probe, as it moved away from the beam source. Interferometer traces illustrating this effect are shown in Fig. 3(b) for the case of He and Ar plasmas. (The corresponding axial wavelengths for these waves were 20 and 200 cm, respectively.) I have also studied the spatial growth rate by modulating the ion beam at different frequencies. As expected, the fastest growth

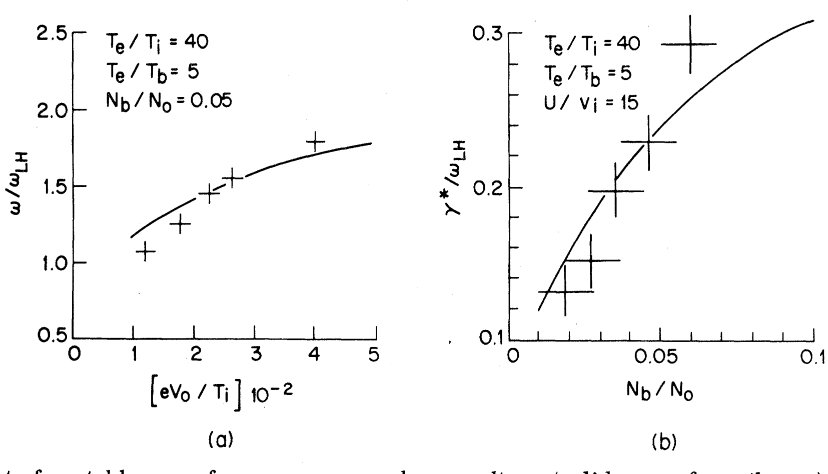

FIG. 4. (a) Plot of unstable wave frequency versus beam voltage (solid curve from theory). (b) Plot of the maximum growth rate versus the beam density (solid curve from theory).

rate occurred when the modulation frequency was close to the most unstable wave frequency excited from background noise by an unmodulated ion beam. As the beam voltage was increased, an increase in the real frequency [see Fig. 4(a)] was observed for the most unstable wave in accord with the linear theory. By pulsing the beam at a fixed accelerating voltage, I was able to measure the temporal growth rate as a function of the beam density. A comparison between the measured values and the theory is shown in Fig. 4(b). As the instability developed into saturation, electron heating was measured. Plasma heating and the associated nonlinear saturation mechanisms will be reported elsewhere.

In conclusion, I have observed the nonresonant lower-hybrid beam-plasma instability in a linear plasma device. The measured properties of the instability agree well with theory. It has been noted that because of this instability, part of the ion-beam energy will be consumed to heat the electrons.

The author acknowledges fruitful discussions with Dr. M. Porkolab and appreciates the able technical assistance received from Mr. T. E. Adams.

[1]T. H. Stix, Plasma Phys. 14, 367 (1972); J. M. Dawson, H. P. Furth, and F. H. Tenney, Phys. Rev. Lett. 26, 1156 (1973); R. F. Post *et al.*, Phys. Rev. Lett. 31, 380 (1973).

[2]H. L. Berk, W. Horton, Jr., M. N. Rosenbluth, and P. H. Rutherford, Princeton Plasma Physics Laboratory Report No. MATT 1127, 1975 (unpublished), and references therein.

[3]J. B. McBride *et al.*, Phys. Fluids 15, 2367 (1972).

[4]T. H. Stix, *The Theory of Plasma Waves* (McGraw-Hill, New York, 1963).

[5]R. P. H. Chang and M. Porkolab, Phys. Rev. Lett. 31, 1241 (1973).

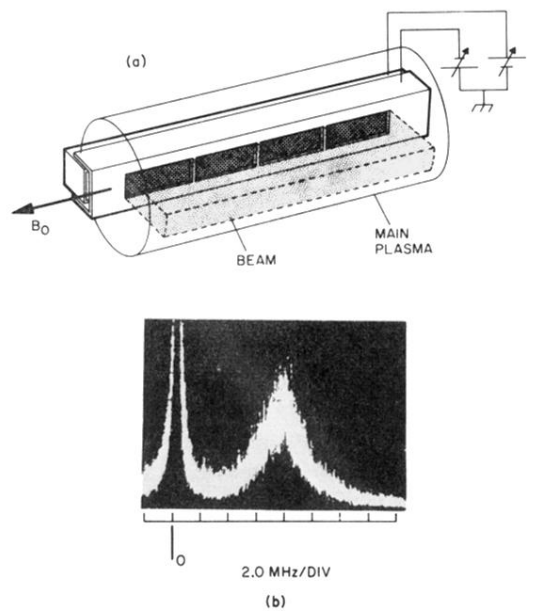

FIG. 2. (a) Simplified schematic of the experimental setup. (b) Instability spectrum for argon plasma.